




Article

d^2 Law and Penetration Length of Jatropha and Camelina Bio-Synthetic Paraffinic Kerosene Spray Characteristics at Take-Off, Top of Climb and Cruise

Sim Sing Mei , Aslina Anjang Ab Rahman , Mohd Shukur Zainol Abidin and Nurul Musfirah Mazlan * 

School of Aerospace Engineering, Engineering Campus, Universiti Sains Malaysia, Nibong Tebal 14300, Pulau Pinang, Malaysia; singmei.9612@gmail.com (S.S.M.); aeaslina@usm.my (A.A.A.R.); aeshukur@usm.my (M.S.Z.A.)

* Correspondence: nmusfirah@usm.my

Abstract: A comparison of d^2 law and penetration length of biofuels with Jet-A through the incorporation of fuel properties and actual combustor inlet data at various flight trajectories is presented. This study aims to identify fuel properties and flight operating conditions that most influence droplet characteristics accurately. The study comprises two phases involving a simulation using GSP to predict combustor inlet data for the respective flight operating conditions and a simulation using ANSYS Fluent V18.1 to obtain combustion characteristics of biofuels and Jet-A. The biofuels chosen in this study are Jatropha Bio-synthetic Paraffinic Kerosene (JSPK) and Camelina Bio-synthetic Paraffinic Kerosene (CSPK), evaluated as pure (100%) and blend (50%) with Jet-A. Thrust specific fuel consumption (TSFC) of biofuels is improved due to lower fuel consumed by the engine. The d^2 law curve shows a heat-up period that takes place at the early stage of the combustion process. The penetration length of the fuels is shorter at take-off. Combusting biofuels reduce combustion temperature and the penetration length of the droplet.

Keywords: penetration length; biofuels; flight trajectory; fuel properties; d^2 law



Citation: Sing Mei, S.; Anjang Ab Rahman, A.; Abidin, M.S.Z.; Mazlan, N.M. d^2 Law and Penetration Length of Jatropha and Camelina Bio-Synthetic Paraffinic Kerosene Spray Characteristics at Take-Off, Top of Climb and Cruise. *Aerospace* **2021**, *8*, 249. <https://doi.org/10.3390/aerospace8090249>

Academic Editor: Cristian Focşa

Received: 29 July 2021

Accepted: 1 September 2021

Published: 4 September 2021

Publisher's Note: MDPI stays neutral with regard to jurisdictional claims in published maps and institutional affiliations.



Copyright: © 2021 by the authors. Licensee MDPI, Basel, Switzerland. This article is an open access article distributed under the terms and conditions of the Creative Commons Attribution (CC BY) license (<https://creativecommons.org/licenses/by/4.0/>).

1. Introduction

In a modernised and busy world, all types of transportation are a crucial way to commute from one place to another. Study shows that road transport, including embedded vehicle and rail transport, contributes to 26–30% and 20–40% of emissions, respectively. Meanwhile, 10–18% of the total emissions is contributed from air transport [1]. In the present day, air transport has become one of the most crucial transportations worldwide. The increasing number of air passengers caused a drastic growth in the aviation sector. According to ICAO's 2019 annual report, the total number of air passengers increased to 4.5 billion in 2019, which is 3.6% higher than the number of passengers in 2018. Due to the high demand, the number of departures increased to 1.7% compared to the previous year, reaching 38.3 million in 2019 [2]. The growth of the aviation sector improves the growth world's economy. However, the growth has led to the increment of greenhouse gas emissions released from the engine into the atmosphere. The increases lead to global warming and the greenhouse effect. Aircraft gas emissions comprise unburnt hydrocarbons, smoke, particulate matter, carbon dioxide, carbon monoxide, and nitrogen oxide that affect human health and the environment [3]. Technology advancements and operational improvements related to aircraft engines, aircraft design, aircraft operations, air traffic management, and fuel sources are the available solutions to alleviate gas emissions and fuel consumption, thus improving energy efficiency.

The aviation industry has identified bio-based aviation fuels as one of the best solutions in alleviating environmental issues [4]. Biofuels have excellent carbon-neutral characteristics and the potential to reduce greenhouse gas emissions, improve waste utilisation,

energy and economic security, and contribute to fuel pluralism [5]. Hydrocarbon-based alternative fuels have been preferred for the replacement of conventional fuel or as a “drop-in” fuel, as they require fewer modifications owing to the interchangeable and compatible properties with traditional jet fuels.

The capability of biofuel in reducing gas emissions is depicted from its combustion characteristics. The combustion characteristics are defined from the quality of the spray, temperature distribution, combustion efficiency, and emission characteristics [3]. Various operating conditions influence combustion characteristics such as fuel used, ambient temperature and pressure, engine power setting, injection pressure, injection timing, spray angle, and many others [6–14]. Fuel properties play a remarkable role in the spray characteristics and emission formation of a gas turbine engine. Fuels with a relatively high density, viscosity, and surface tension could delay the atomisation process [15]. The low viscosity and specific heat capacity of biofuels accelerate the combustion process and fuel evaporation in the combustion chamber.

Compared to kerosene, the low viscosity of ethanol and methanol tends to have proper atomisation without the need to preheat the fuel [16]. Rapid combustion can improve engine efficiency, thus reducing emissions from aircraft engines. Apart from viscosity, caloric value, density, vapour pressure, and volatility also contribute to atomisation quality. The lower viscosity and caloric value of biofuels are easy to atomise at low temperatures and provide short penetration. Studies showed that ethanol evaporates fastest owing to its high volatility, whereas biodiesel evaporates the slowest due to its relatively small vapour pressure. The lowest evaporation of biodiesel implies the most extended spray penetration [6,17]. The faster evaporation of biofuels promotes a proper fuel-air mixture of combustion, thus leads to a better combustion efficiency [18].

Besides fuel properties, operating conditions also influenced the performance of the combustion. Shameer and Ramesh [9] observed enhanced atomisation, air–fuel mixture, and combustion as they tested the injection timing and injection pressure on a biodiesel engine. The air–fuel mixture improves as the injection pressure increases, owing to the wide surface area of the fuel droplet that interacts with the hot air in the chamber, which consequently improves combustion efficiency [10]. Zhu and Luo [11] found that the size of the fuel droplets was reduced as the spray angle increases, thus increasing penetration depth and the span-wise angle and expansion area of the fuel droplet.

Synthetic Paraffinic Kerosene (SPK) and Hydro-processed Ester and Fatty Acid (HEFA) have been approved by the American Society for Testing and Materials (ASTM) for use as aviation fuel. However, the fuel has to be blended with Jet-A for up to 50% [19]. Jatropha, Camelina, and Algae are amongst the plant sources that have been used as feedstock in developing SPK fuel. These plants are non-food energy crops, thus do not compete with food crops, yet show excellent potential in the transportation field [20]. The SPK fuel is developed through the conversion of feedstock’s free fatty acids into shorter diesel-range paraffin. The SPK fuel has similar types of molecules as those in Jet-A [21]. The fuel is blended with Jet-A to improve engine performance and reduce NO_x due to its combustion’s lower flame temperature [19]. However, the relatively low flame temperature increases the CO formation due to the incomplete combustion [21].

Previous studies on Jatropha and Camelina derived alternative fuel mainly focus on engine performance and the formation of NO_x and CO emissions, particularly at specific operating conditions. Jatropha Bio-synthetic Paraffinic Kerosene (JSPK) and Camelina Bio-synthetic Paraffinic Kerosene (CSPK) provide increment in engine thrust due to the higher heating value of the fuels [22]. Mazlan and Savill [21] used a simple 0D aircraft engine emission model called HEPHAESTUS to compare NO_x and CO emissions of JSPK and CSPK with Jet-A at cruise conditions. Lower NO_x was obtained due to the lower temperature of the combustion. The lower combustion temperature observed in this work is the main factor that leads to higher CO as a colder temperature produces incomplete combustion. Other criteria influencing CO formation, such as evaporation rate and spray penetration, were not observed. The evaporation process and spray penetration of JSPK and CSPK were

evaluated in Lim and Razak [6] at spray cone angles ranging from 30–50 degrees and at injection pressures of 1–10 bar. The evaluation was performed in a spray model developed based on droplet motion, energy equation, and boiling mass transfer obtained from ANSYS Fluent guidelines. The droplet experienced faster evaporation during the initial period and did not exhibit a heat-up period. A strong dependence between evaporation time and vapour pressure was observed. Air density was assumed constant throughout the process. Therefore, the influence of fuel density on the spray penetration was pronounced.

Moreover, the larger spray cone angle was required for high viscous fuel for better fuel–air-mixing inside the chamber. Another study on Jatropha-derived alternative fuel was performed in Sivakumar and Vankeswaram [23] who tested the fuel on a simplex swirl atomiser. They observed identical secondary atomisation features of Jatropha fuel with Jet–A. Rapid evaporation of the fuel suggests marginal decreases in the Sauter mean diameter (SMD) of the fuel. Hashimoto and Nishida [24] investigated NO_x and CO formation of Jatropha experimentally as a function of adiabatic flame temperature and equivalence ratio. The fuel was tested in the form of pure oil and methyl ester. Low vapourability of Jatropha pure oil causes decreases in reaction time, thus a reduction of CO formation. They also observed a significant impact of airflow but a minimal impact of fuel flow rate or fuel viscosity on the NO_x formation.

Although researchers have conducted numerical and experimental studies on the combustion characteristics of Jatropha and Camelina derived fuels, combustion characteristics of the fuels at various flight operating conditions are still lacking in the literature. The previous studies focused only on a specific condition without considering other parameters to represent actual flight conditions. Therefore, this study is performed as an extension to work by Mazlan and Savill [21], who evaluated the fuels at one particular flight condition, which is the cruise. The work observed that a reduction in flame temperature was the main factor that caused the increment of CO without further analysis of droplet characteristics on the CO formation. Therefore, this study compares droplet characteristics of Jatropha and Camelina-derived alternative fuel at take-off, TOC, and cruise. The study was performed by varying the critical parameters such as fuel properties, temperature, pressure, fuel, and mass flow representing the actual aircraft flight trajectory. It is hypothesized that the combination of fuel properties and flight operating condition parameters may influence the spray characteristics as they will influence flow behaviour inside the chamber. Therefore, the present study aims to fulfil two research objectives:

1. To measure combustor inlet data at the selected flight trajectories.
2. To identify fuel properties and flight operating conditions that most influence the droplet characteristics accurately.

The first objective is achieved by evaluating the aircraft engine using the Gas Turbine Simulation Program (GSP) to obtain the actual value of pressure, temperature, total air mass flow, and fuel flow entering the combustion chamber. The simulation is performed for take-off, top of the climb (TOC), and cruise. Combustor inlet parameters obtained from GSP are taken as input to ANSYS Fluent in conjunction with properties of the biofuels to accomplish the second objective. Biofuels, namely Jatropha Bio-synthetic Paraffinic Kerosene (JSPK), and Camelina Bio-synthetic Paraffinic Kerosene (CSPK), are tested as pure and blend with Jet–A. The combustion chamber used for evaluation was based on the combustion chamber used in Mark and Selwyn [25]. Mesh independence analysis was performed to identify the best mesh to capture the correct combustion process. The present study visualised spray characteristics of the fuels focusing on the changes of droplet size and penetration of the spray at the selected flight operating conditions.

2. Materials and Methods

The present study is performed in two parts. The first part involved a numerical simulation using the Gas Turbine Simulation Program (GSP) and the second part involved a numerical simulation using ANSYS Fluent. GSP is a computer tool developed by the Netherlands National Aerospace Laboratory (NLR) and the Delft University of Technology

to calculate the thermodynamic cycle and performance analysis of the gas turbine. The software is developed based on a 0D-modelling of the gas turbine thermodynamic cycle. It implies an average flow property over the cross-section areas at the inlet and the exit of the engine component models. The engine components such as inlet, compressor (s), combustor, turbine (s), duct, and exhaust are arranged to create the engine thermodynamic cycle. The component parameters such as efficiency, pressure ratio, and shaft speed are required to be input into the tool.

The second phase involves a combustion simulation using ANSYS Fluent. ANSYS Fluent is a fluid simulation software to visualise and solve problems related to fluid flow. The combustion is modelled in a cylindrical chamber based on Mark and Selwyn [25]. Droplet behaviour is evaluated by cooperating data obtained from GSP simulation.

2.1. Fuels for Evaluation

Two biofuels were used in this study, namely Jatropha Bio-synthetic Paraffinic Kerosene (JSPK) and Camelina Bio-synthetic Paraffinic Kerosene (CSPK). Meanwhile, Jet-A was used as the baseline fuel. JSPK and CSPK were developed from Jatropha and Camelina plants, respectively. The plant oil was converted to Bio-synthetic Paraffinic Kerosene through a hydro-treated chemical process that converts triglyceride and fatty acids in the oil into the same type of molecules present in Jet-A. As a result, the fuels have almost similar properties to Jet-A. Therefore, implementing these fuels in the current gas turbine engine is promising without considering any significant modification to the combustion chamber system and configuration. The properties of the biofuels are shown in Table 1. In addition, the blend of JSPK and CSPK with 50% Jet-A were also evaluated to identify the effect of blended fuel on combustion performance. The blend of 50% JSPK with 50% Jet-A is denoted as B50JSPK, while B50CSPK is used to denote the blend of 50% CSPK with 50% Jet-A.

Table 1. Fuel properties data from Mazlan and Savill [22] Kinder and Rahmes [26].

Fuels Properties	Jet-A (Baseline Fuel)	JSPK	CSPK	B50JSPK	B50CSPK
% C (approx.)	85.8	85.4	85.4		
% H (approx.)	14.2	15.1	15.5		
% N (approx.)	n/a	<0.10	<0.10		
C/H	5.2	5.7	5.5		
Molecular formula (approx.)	C ₁₂ H ₂₃	C ₁₂ H ₂₆	C ₁₂ H _{25.4}	C ₁₂ H _{24.5}	C ₁₂ H _{24.2}
Molecular weight (g/mol)	167	170	169.4	168.5	168.2
Specific Heat, C _p (J/kg·K)	2093	2132	2135	2113	2114
Density at 15 °C (kg/m ³)	775–840	749	753	762	764
Viscosity at −20 °C (mm ² /s)	8.0	3.663	3.336	5.832	5.668
Net heat of combustion (MJ/kg)	42.8	44.3	44.0	43.55	43.4
Enthalpy of formation (kJ/mol)		−330.5	−335.45		
Boiling Temperature (K)	573.15	528.15	524.15	550.65	548.65

The properties of the Jet-A, JSPK, and CSPK were obtained from Kinder and Rahmes [26] and Mazlan and Savill [22], while properties of the blend fuels (B50JSPK and B50CSPK) were obtained through an estimation using a general equation of mixture shown in Equation (1) as also considered in [27].

$$Properties_{mix} = \sum x_i Properties = x_1 Properties_1 + x_2 Properties_2 \quad (1)$$

2.2. Flight Conditions for Evaluation

Based on the International Civil Aviation Organization (ICAO), an aircraft Land and Take-off (LTO) cycle consist of Take-off, Top of Climb (TOC), Cruise, and Taxi/ground idle, which is represented based on the percentage of maximum thrust. Take-off, climb, and cruise are the operating modes that significantly impact the combustion characteristics. Therefore, these three operating modes as shown in Table 2 were selected for evaluation.

Table 2. Flight conditions detail.

Flight Conditions	Altitude (m)	Mach Number	HPT Shaft Speed (%)
Take-off	0	0	105
TOC	10,668	0.8	100
Cruise	10,668	0.8	95

2.3. Engine Performance Set-Up in GSP

The GSP simulation was performed using a high-bypass turbofan aircraft engine model—Bigfan.mxl available in GSP sample projects (Figure 1). The engine consists of a fan, a low-pressure compressor (LPC), a high-pressure compressor (HPC), a combustor chamber (CC), a high-pressure temperature (HPT), and a low-pressure turbine (LPT). The high-bypass turbofan engine plays a pivotal role in the flight capabilities of modern aircraft [28]. The CFM 56 is an example of high-bypass turbofan engine manufactured by General Electric (USA) and Safran Aircraft Engines (France). The engine is preferred over conventional turbojet engines as it improves fuel efficiency and noise level. In addition, the engine is efficient when flying up to Mach number 0.85. The characteristics of the engine are given in Table 3.

The engine's performance at the three operating modes, Take-off, TOC, and Cruise, was evaluated based on operating modes shown in Table 2. The engine model was set to operate at 105% shaft speed for take-off, 100% shaft speed for TOC, and 95% shaft speed for the cruise. During take-off, the aircraft operated at a static condition where the altitude is 0 m and at 0 Mach number. Meanwhile, the ambient condition of the aircraft was set to 10,668 m altitude and 0.8 Mach number when the aircraft was at TOC and cruise. A rotor speed controller as shown as "Rotor speed ctrl" in Figure 1 was used to control the shaft speeds. An "operating envelope scheduler" was used to generate ambient conditions to represent the operating modes. In this simulation, TOC condition was set as design point while take-off and cruise were set off-design.

Table 3. Engine characteristics adapted from Gaspar and Sousa [29].

Parameter	Value
Bypass pressure ratio (BPR)	5.7
Fan pressure ratio	1.7
HPC pressure ratio	6.0
LPC pressure ratio	2.0
Fan efficiency	0.86
HPC efficiency	0.88
LPC efficiency	0.88
CC efficiency	0.995
HPT efficiency	0.89
LPT efficiency	0.87

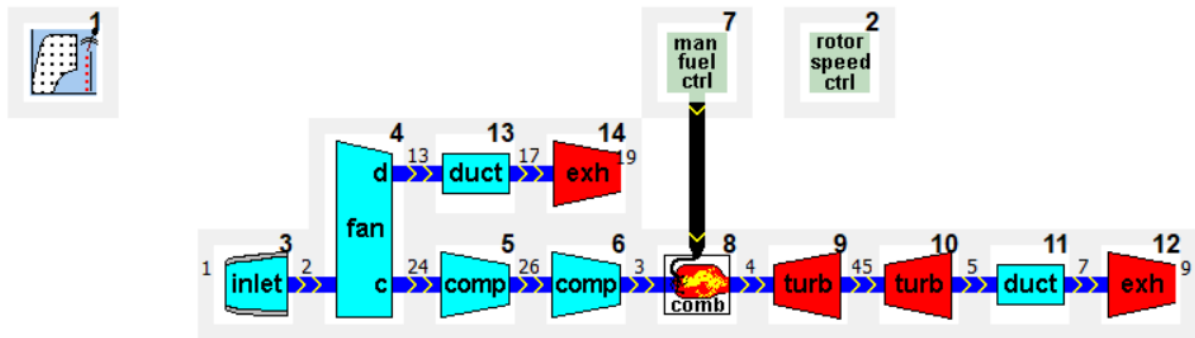


Figure 1. Configuration of high bypass turbofan engine modelled in GSP. Station 4 (Fan), Station 5 (LPC), Station 6 (HPC), Station 8 (CC), Station 9 (HPT) and Station 10 (LPT).

2.4. Combustion Performance in ANSYS Fluent

2.4.1. Combustor Geometry and Mesh Independence Analysis

The combustor chamber was modelled based on the combustor geometry available in the literature [25]. The chamber was a cylindrical shape, as displayed in Figure 2a. The total length of the chamber was 160 mm, and the diameter of the combustion chamber was 44.3 mm. The chamber was divided into a primary zone, secondary zone, and dilution zone. The length of each zone was 30.20 mm, 20.13 mm, and 109.67 mm, respectively. Each zone was provided with the main holes and cooling walls. There were 40 main holes in the primary zone, and 20 main holes in the secondary and dilution zones, respectively. The main hole's diameter was 20 mm. The cooling wall for each zone was presented as a strip line. The length of the cooling wall for the primary zone was 4 mm, 2.4 mm for the secondary zone, and 693 mm for the dilution zone. Figure 2b displays the mesh of the combustion chamber model using a polyhedral mesh. The mesh was selected as it produces a reliable result with a lower cell count compared to tetrahedral mesh [30].

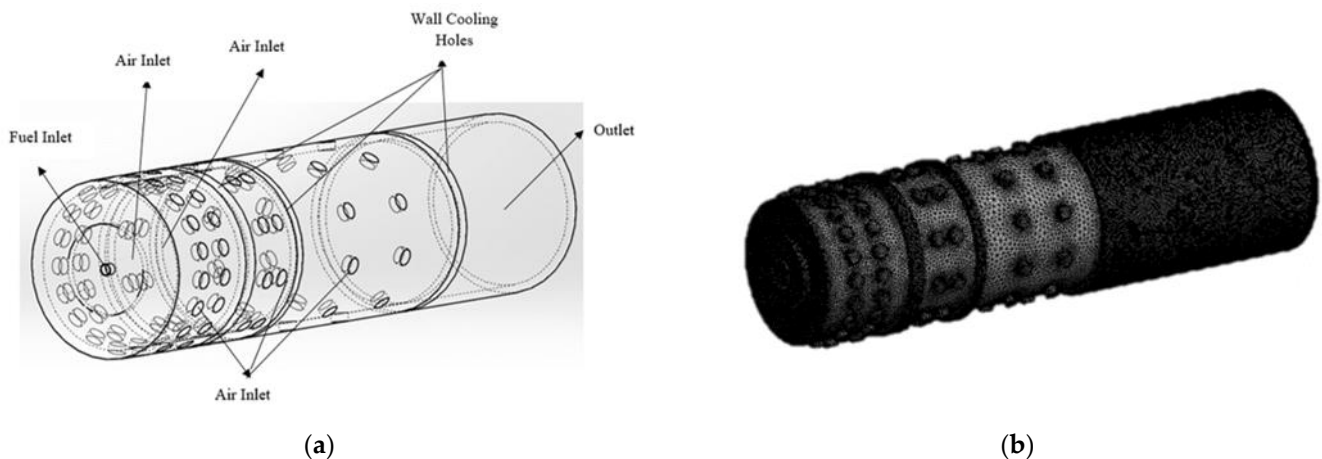


Figure 2. (a) The Geometry of the Combustor Chamber. (b) The Polyhedral Mesh of the Combustor Chamber.

Mesh independence analysis plays an essential role in determining accurate results. Table 4 shows three different meshes created for the combustor. All the meshes were evaluated by using boundary conditions considered in Mark and Selwyn [25]. In their study, the air mass flow rate at the combustor inlet was taken as 28.7103 kg/s. The inlet temperature and pressure were taken as 743.352 K and 2,083,450 Pa, respectively. Fuel mass flow rate was 0.25818 kg/s, and the swirl velocity was taken as 30 m/s. The fuel used for validation is Jet-A. All the meshes were validated by comparing the percentage difference of the maximum temperature obtained in the present study with the maximum temperature obtained from Mark and Selwyn [25]. A convergence limit of 10^{-6} was set. Coarse mesh

gives a short computational time, but the results obtained are poor compared to medium and fine. Medium mesh provides an improvement to the accuracy with a considerable computational time. However, fine mesh provides better accuracy, which was closer to the reference value. Computational time consumed for fine mesh is still acceptable. Finally, a fine mesh is selected to perform the numerical calculation.

Table 4. Grid independence analysis based on computational time and percentage difference with the reference value.

Mesh Type	Element Number	Maximum Temperature	Computational Time	% Difference Wrt MarkandSelwyn [25]
Coarse	365,521	2531.49	20 min, 36 s	2.0
Medium	3,577,388	2536.42	1 h 30 min	1.8
Fine	6,430,906	2561.95	7 h	0.8

2.4.2. Boundary Conditions for the Simulation

The numerical simulation of the combustion was performed using ANSYS Fluent. The simulation was solved in fully three-dimensional (3D), steady, Reynolds averaged, and Navier–Stokes equations. The pressure-based algorithm was used to solve the equation. The standard k-epsilon turbulence model was chosen and solved by the SIMPLE solution method. The near-wall flow was neglected, and the second-order upwind model was adopted. The particle trajectory was solved using a discrete phase model (DPM). The surface injection type was implemented in the simulation where the fuel was injected through the surface of the fuel inlet. The Rosin–Rammler method was selected for the fuel particles' diameter distribution. Particle diameters were varied between 0.0001 m and 1 µm. The droplet was assumed as a sphere. The fuel temperature was set as 288.15 K and no preheat temperature was set for the fuels. The eddy-dissipation model was adopted as the turbulent-chemistry model. Due to the limitation of the chemical reaction of biofuel, the combustion of the fuel was modelled by considering a global one-step reaction mechanism that assuming the complete conversion of the fuel–air mixture to CO₂ and H₂O. Table 5 shows the one-step reaction equation of the fuels tested in this study.

Table 5. One step global chemical reaction for each tested fuel.

Fuels	One-Step Reaction Equation
Jet-A	$C_{12}H_{23} + 17.75O_2 \rightarrow 12CO_2 + 11.5H_2O$
JSPK	$C_{12}H_{26} + 12.5O_2 \rightarrow 12CO_2 + 13H_2O$
CSPK	$C_{12}H_{25.4} + 12.35O_2 \rightarrow 12CO_2 + 12.7H_2O$
50JSPK	$C_{12}H_{24.5} + 12.13O_2 \rightarrow 12CO_2 + 12.25H_2O$
50CSPK	$C_{12}H_{24.2} + 12.05O_2 \rightarrow 12CO_2 + 12.1H_2O$

3. Results and Discussion

This section presents a discussion of the results obtained from the simulation. All results presented in this section are instantaneous, where it is extracted in every model and simulation accordingly. The results are presented by comparing the biofuels data with Jet–A. The comparison was made by calculating the percentage difference between biofuels data to Jet–A as shown in Figures 3–5. Meanwhile, some results are presented by comparing the data directly, as shown in Figures 6–9.

3.1. Comparison of Combustor Inlet Parameter

Figure 3 compares air pressure, airflow, fuel flow, and air temperature between biofuels with Jet–A. The comparison was based on the percentage difference of the biofuel to Jet–A. Compared to Jet–A, the air pressure delivered by the compressor to the combustor inlet for

all biofuels reduces during TOC and cruise. However, the air pressure at the combustor air inlet for B50JSPK and B50CSPK increases during take-off. It is also noticed that the airflow and air temperature also increase. In contrast, the lower fuel consumption is observed for all biofuels at all flight conditions. For all tested fuels, data at the combustor inlet are higher when the engine was at take-off where the shaft speed was at the maximum power, while a slight difference is observed for TOC and cruise. It is noticed that ambient conditions at TOC and cruise is similar for both flight conditions. The only difference observed between TOC and cruise is mainly on the shaft speed. The shaft speed at TOC is 100%, while it is 95% at cruise. This 5% difference does not provide a significant impact on the pressure, temperature, airflow, and fuel flow difference at the combustor inlet.

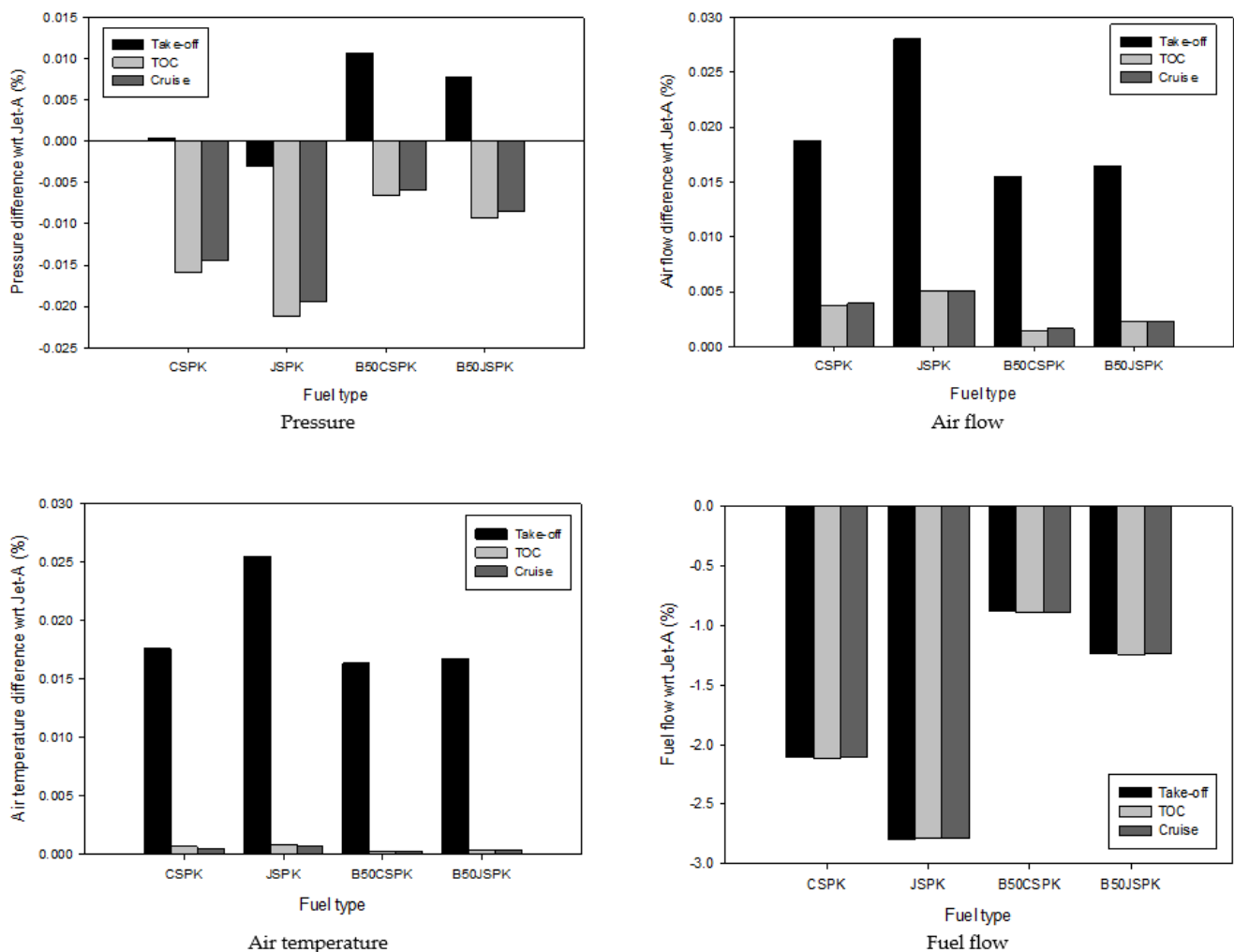


Figure 3. Comparison of pressure, airflow, air temperature, and fuel flow of biofuels with Jet-A.

3.2. Engine Performance Analysis

The engine thrust and thrust-specific fuel consumption (TSFC) of the biofuels during take-off, cruise, and TOC are observed. Figure 4 depicts the percentage difference of thrust produced from biofuels to Jet-A. The result shows that the biofuels produced more thrust than Jet-A during take-off, but the lower thrust was produced during cruise and TOC. Thrust increases around 0.015% at take-off but reduces to 0.035% at TOC and cruise. A similar observation was also noticed in Mazlan and Savill [21]. However, the increment of thrust is the highest for B50CSPK. During take-off, the engine was operated at full throttle, requiring the engine shaft to rotate at the maximum capacity. As a result, the thrust produced is higher compared to other flight conditions. The generation of thrust is usually associated with the heat of combustion. All biofuels tested in this study

have a higher heat of combustion compared to Jet-A, and thus produce higher thrust. Although JSPK has the highest heat of combustion amongst other biofuels, the lowest thrust is obtained. This finding identifies that despite the heat of combustion, other fuel properties may influence the production of engine thrust.

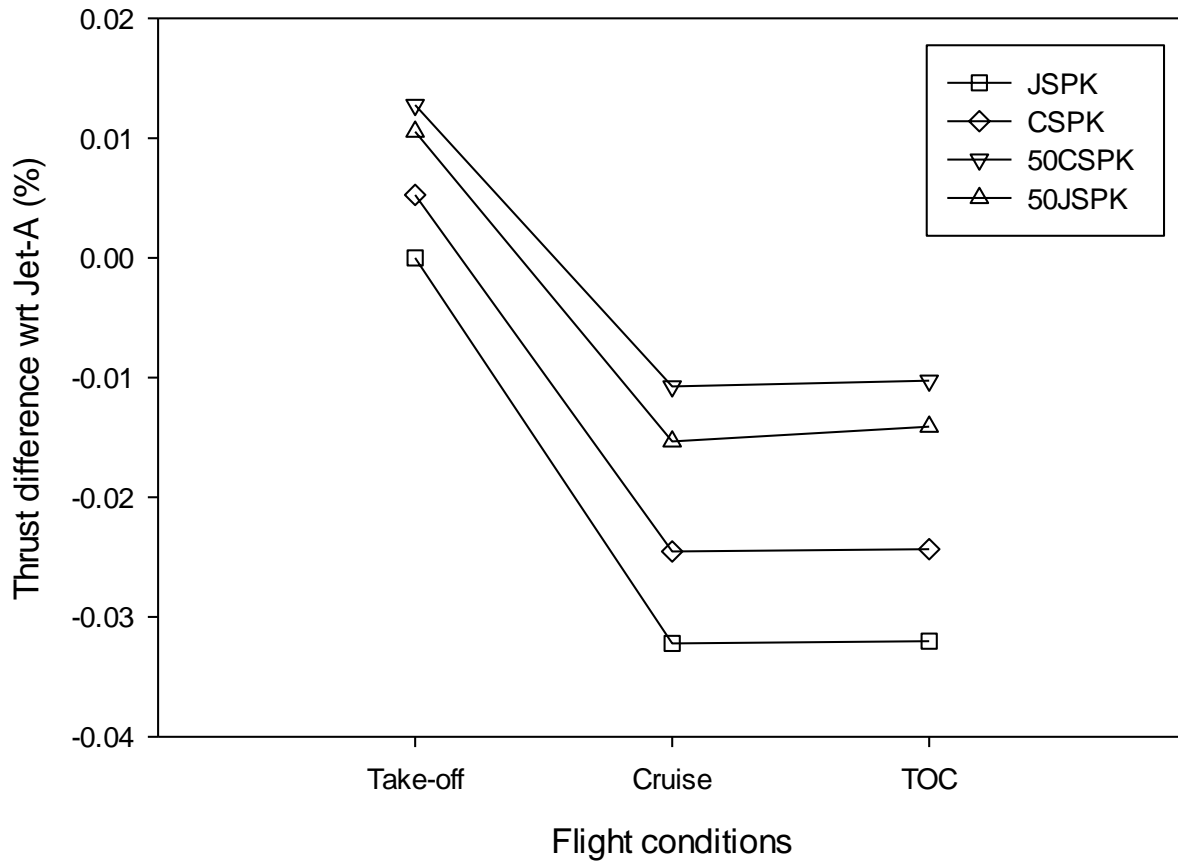


Figure 4. Thrust difference of biofuels compared to Jet-A.

According to Mattingly [31], the total thrust (F) of a turbofan is a combination of thrust from the fan section (F_{fan}) and thrust from the core engine (F_{Core}) (Equation (2)). The thrust of each section (fan and core) was derived from the multiplication of the mass flow rate of each section with a difference between initial velocity (V_0) and velocity at the fan nozzle (V_{19}) and velocity at the core engine nozzle (V_9) as shown in Equation (3) and Equation (4). The exit velocity of the core engine can be presented in terms of the ratio of the burner exit enthalpy to the ambient enthalpy (τ_λ), compressor temperature ratio (τ_c), total to static temperature ratio of the free stream (τ_r), and turbine temperature ratio (τ_t), as shown in Equation (5).

$$F = F_{Core} + F_{fan} \quad (2)$$

$$F_{core} = \dot{m}_{Core}(V_9 - V_0) \quad (3)$$

$$F_{fan} = \dot{m}_{Fan}(V_{19} - V_0) \quad (4)$$

$$\frac{V_9}{a_0} = \sqrt{\frac{2}{\gamma - 1} \frac{\tau_\lambda}{\tau_r \tau_c} (\tau_r \tau_c \tau_t - 1)} \quad (5)$$

The turbine temperature ratio (τ_t) in Equation (5) is obtained from the energy balance equation of the turbine work as shown in Equation (6).

$$W_t = (\dot{m}_c + \dot{m}_f) c_p (T_{t4} - T_{t5}) \approx \dot{m}_0 c_p T_{t4} (1 - \tau_t) \quad (6)$$

From the equation, the turbine work was contributed to by the temperature difference between turbine inlet (T_{t4}), turbine outlet (T_{t5}), and heat capacity (c_p) of the fuel. The equation shows that the higher fuel capacity of CSPK exhibits higher thrust than JSPK.

Figure 5 shows the TSFC percentage difference of the biofuels compared to Jet-A at the tested flight operating conditions. TSFC was determined by the ratio of fuel flow to the total thrust of the engine. The TSFC of the engine reduces as biofuels were used in the engine. JSPK was found to have the highest reduction in TSFC compared to other biofuels. At a particular flight condition, although biofuels produce higher thrust compared to Jet-A, the percentage thrust difference of the biofuels is relatively small. At this slight difference in engine thrust, the reduction in TSFC is proportional to less fuel consumed by the engine as biofuels used in the engine. The TSFC of the engine is consistent with the amount of fuel used, as shown in Figure 3. The engine consumed less fuel when operated with JSPK than other biofuels because of the low density of the fuel (refer to Table 1). The fuel consumed by JSPK is 2.86% lower which resulted from a 3.35% lower density compared to Jet-A.

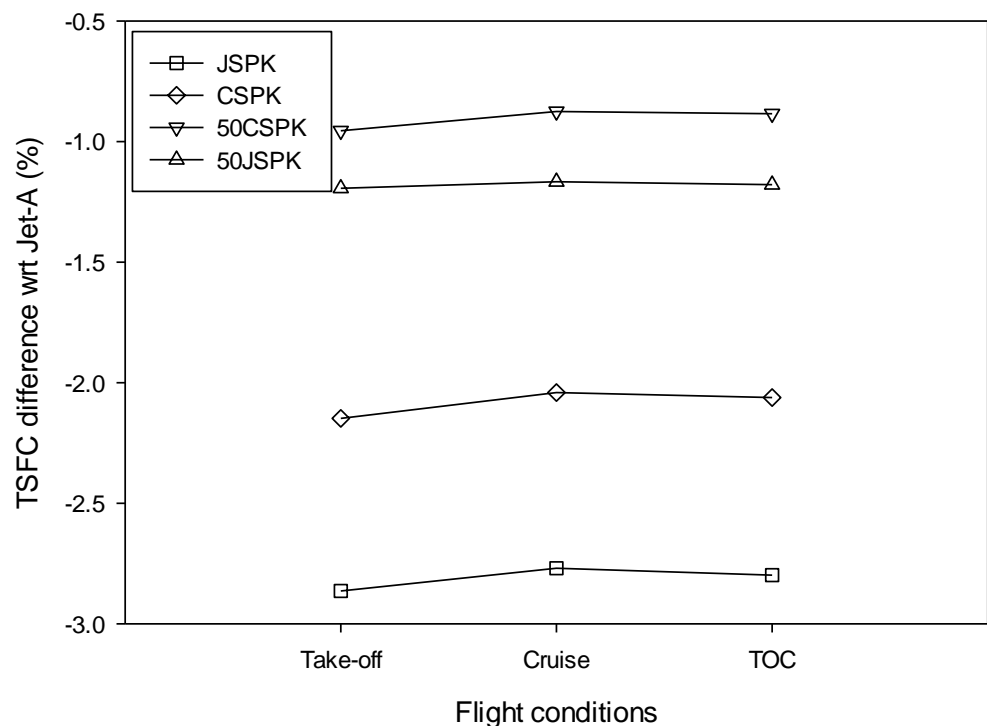


Figure 5. TSFC difference of biofuels compared to Jet-A.

3.3. Combustion Characteristics Evaluation

3.3.1. Comparison of d^2 Law between Jet-A and Biofuels

Figure 6 shows the d^2 law curve, which indicates droplet behaviour during the vaporisation process. In our study, the droplet was injected via surface injection in which the initial droplet sizes were set between 0.0001 m to 1 μm . For comparison purposes, an initial droplet diameter of 12 μm was selected for all fuels and cases. Insignificant changes in droplet diameter were observed for Jet-A and biofuels at the early stage of the evaporation process due to the heating-up period. After the initial heating-up period, a rapid reduction in the droplet can be seen as the fuel reaches the fuel's boiling temperature. The heating-up period was observed for all flight operating conditions. The d^2 law curves for TOC and cruise are identical while a significant difference in d^2 law curve was found for take-off.

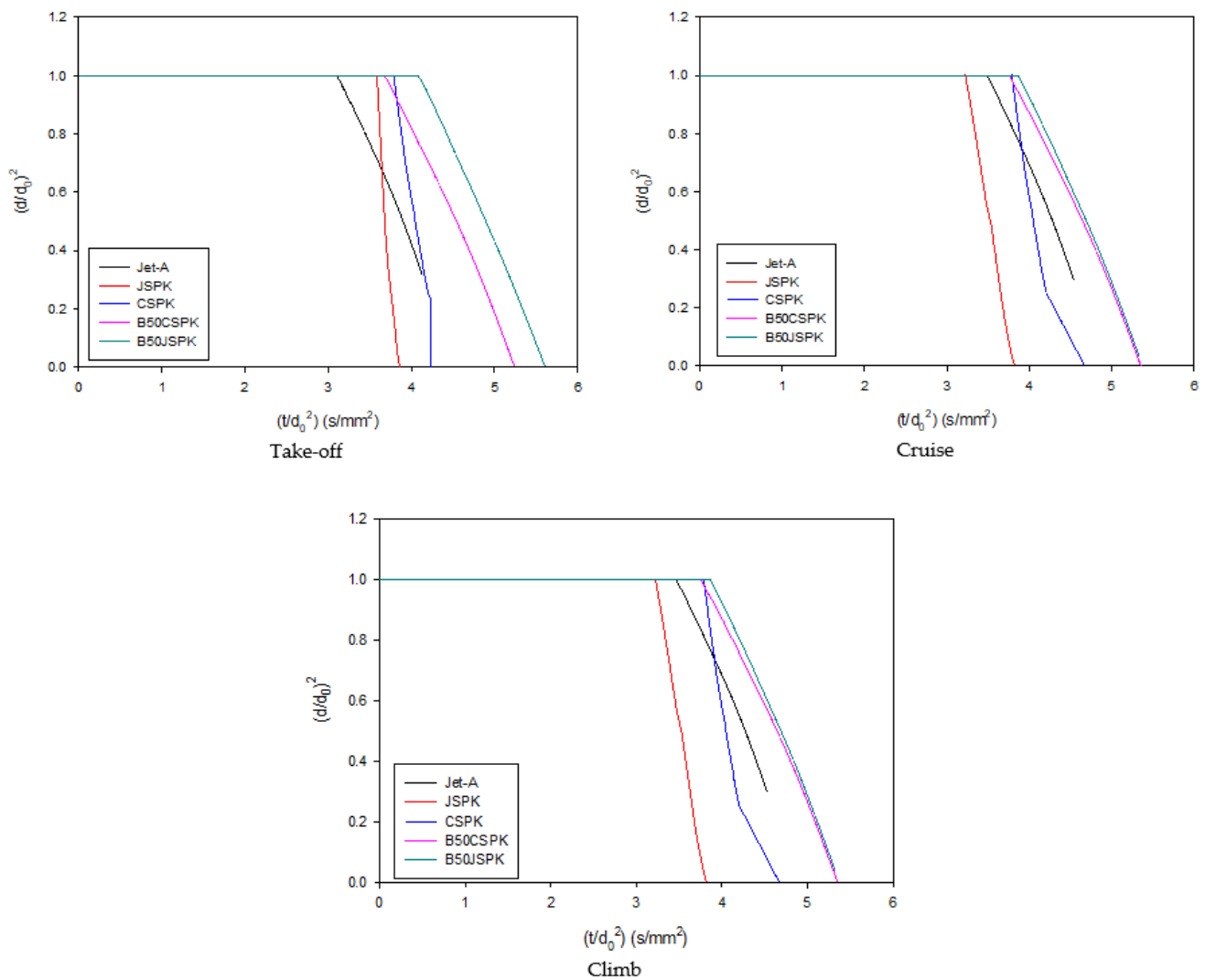


Figure 6. Comparison of d^2 law curve of biofuels and Jet-A at Take-off, TOC, and Cruise.

Figure 7 shows the time taken by the droplet during the heat-up. The heat-up period in this present study is determined from the time start of injection (t_{soi}) until the time of the droplet starts to decrease. The heat-up period of Jet-A, CSPK, and B50CSPK increases as the aircraft reaches cruise and TOC from take-off, but vice versa for JSPK and B50JSPK.

The time required for JSPK, CSPK, B50CSPK, and B50JSPK to start to atomise during take-off are 516.8 μs , 519.5 μs , 532.01 μs , and 590.06 μs , respectively. This time duration depends on fuel properties and combustor inlet condition. Volatility, boiling temperature, and density are the fuel properties that influence the evaporation and vaporisation process of the particle [6]. Fuel with a low boiling temperature is more volatile and has higher vapour pressure compared to fuel with a higher boiling temperature, thus encourages the vaporisation process. In addition, fuel with a higher boiling point requires a longer time to reach the respective boiling temperature. Jet-A has the highest boiling temperature among all tested fuels; less volatility thus results in lower vapour pressure. The effect of boiling temperature on the vaporisation process is observed during TOC and cruise, where the heat-up period for Jet-A is longer compared to JSPK, but still smaller than CSPK. Unfortunately, the effect of boiling temperature on the heat-up period is not observed during take-off conditions. Although the boiling temperature of biofuels is lower than Jet-A, the heat-up period of biofuels is longer than that of Jet-A. The effect of boiling temperature on the vaporisation process is more significant after the heat-up period.

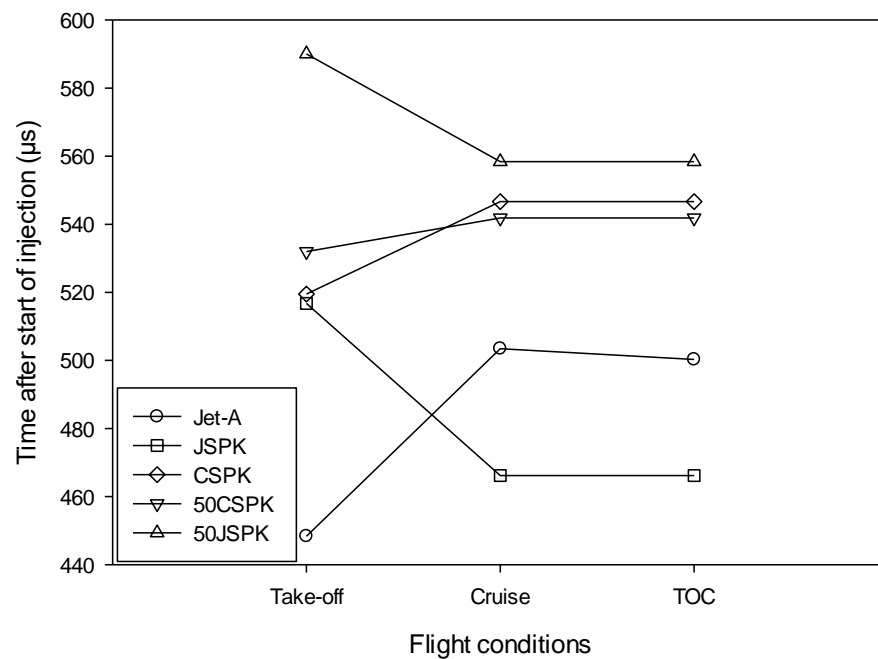


Figure 7. Comparison of the heating-up period of biofuels and Jet-A.

In addition to fuel properties, the effect of combustor inlet data on the heat-up period is remarkable during take-off and vice versa for cruise and TOC. During take-off, the engine is operated at a low Mach number ($M = 0$) and static ambient conditions (altitude = 0 m). The engine operates at TOC and the cruise has a higher Mach number ($M = 8$) and altitude (altitude = 106,880 m). As a result of altitude and speed differences, the inlet conditions of the combustor, such as air pressure, air temperature, and airflow entering the chamber, were varied, thus influencing the heat-up period of the fuel droplet. The fuel's time during the heat-up period is insignificant, particularly when the engine is in cruise and TOC. The slight difference in the value obtained between TOC and cruise is mainly due to the slight difference in HPT rotational speed between these flight operating conditions (Figure 3).

In this present study, combustor inlet conditions such as air pressure, air temperature and air mass flow are observed to influence the vaporisation and evaporation process of the fuels. It is noticed that the heat-up period increases with the air pressure but reduces with increases in air temperature. This observation is also consistent with [32]. For the case of JSPK, although the air temperature for JSPK is the highest amongst other fuels, decreases in air pressure are dominant, causing the heat-up period of the fuel to be longer than other fuels. The higher air temperature of JSPK contributes to the fastest droplet reduction among other fuels. Higher air temperature at the combustor inlet is beneficial as it transfers the heat to the droplet, thus helping the droplet to reach its boiling temperature faster. A similar trend was observed for CSPK.

The reduction of the droplet's diameter is evidenced when referring to the temperature variation along the centre line of the combustor (Figure 8). In this study, all fuels' temperature was set as 288 K. No preheat temperature was set for the fuels. It is observed that insignificant temperature changes are observed near the combustor inlet, leading to insignificant changes in the particle's size particularly during the heat-up period. Later, increases in the particle's temperature are observed due to heat transferred by the surrounding air causes reduction of the particle's size. As observed in Figure 8, the temperature of the JSPK particle is slightly higher than Jet-A at the beginning of the evaporation process. As a result, the time required of JSPK during the heat-up period is shorter than Jet-A.

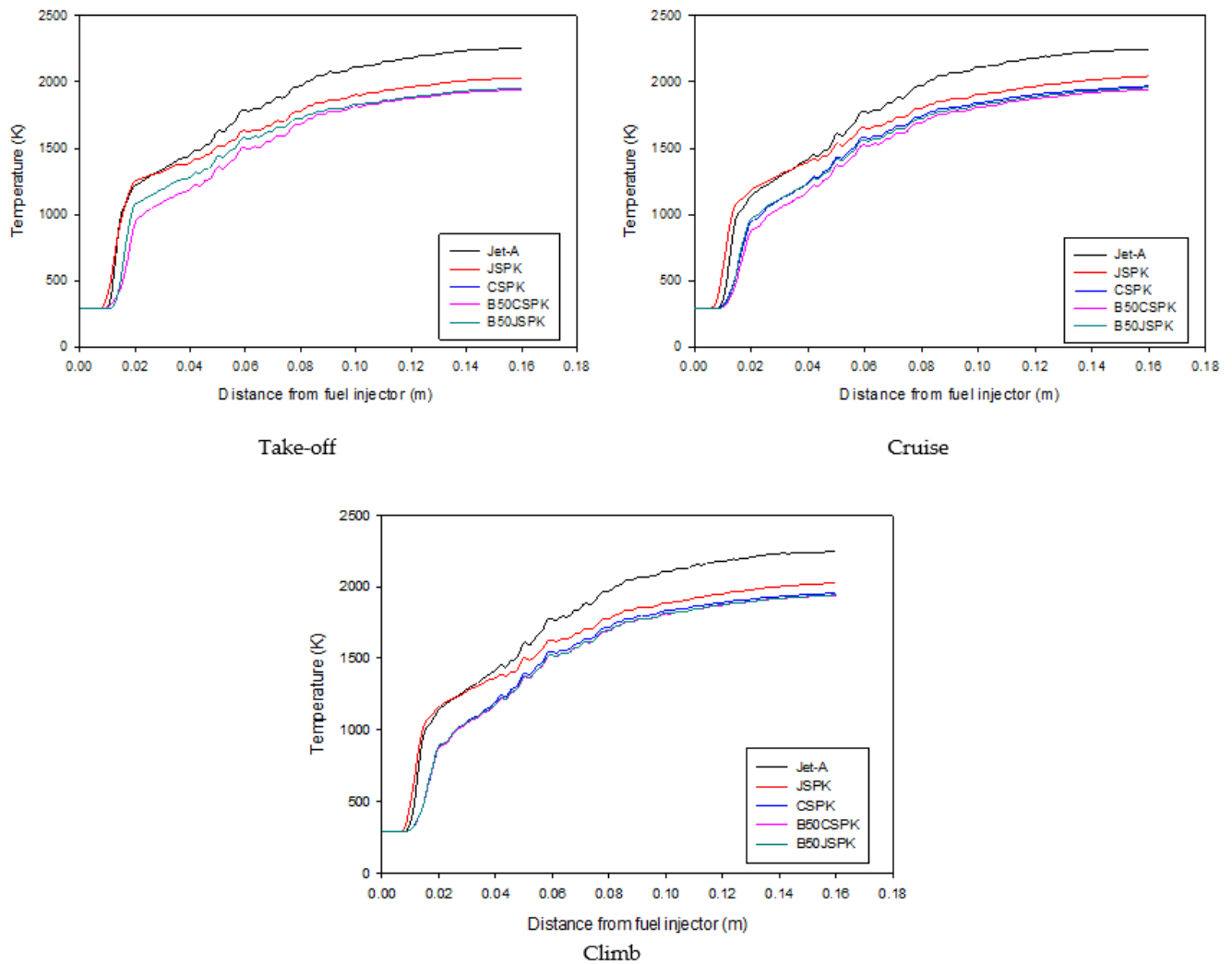


Figure 8. Temperature variation along the x -axis of the chamber.

By comparing the maximum temperature of all fuels at a particular flight operating condition, the maximum temperature recorded for biofuels is between 12–15% lower than Jet-A when the aircraft is at take-off and 12–14% lower than Jet-A when the aircraft flies at TOC and cruise. The lower temperature observed for biofuels is expected to reduce the generation of nitrogen oxide (NO_x) as the production of NO_x is mainly associated with combustion temperature. On the other hand, this lower temperature increases carbon monoxide production (CO) due to incomplete combustion.

3.3.2. Comparison of Penetration Length of Biofuels with Jet-A

In order to further analyse factors that influence CO formation, a comparison of penetration length is presented. Spray penetration is the maximum distance of the spray as it is injected into stagnant or flowing air. The penetration corresponds to the kinetic energy of the droplets and the aerodynamic resistance of the surrounding gas. Over-penetration of the spray leads to impingement of the fuel on the combustor chamber walls, while inadequate penetration leads to unsatisfactory fuel-air mixing with consequent CO emissions. The penetration of the droplet during take-off, cruise, and TOC is shown in Figure 9. All biofuels penetrate between 2–76% lower than Jet-A at take-off and up to 83% lower than Jet-A at TOC and cruise.

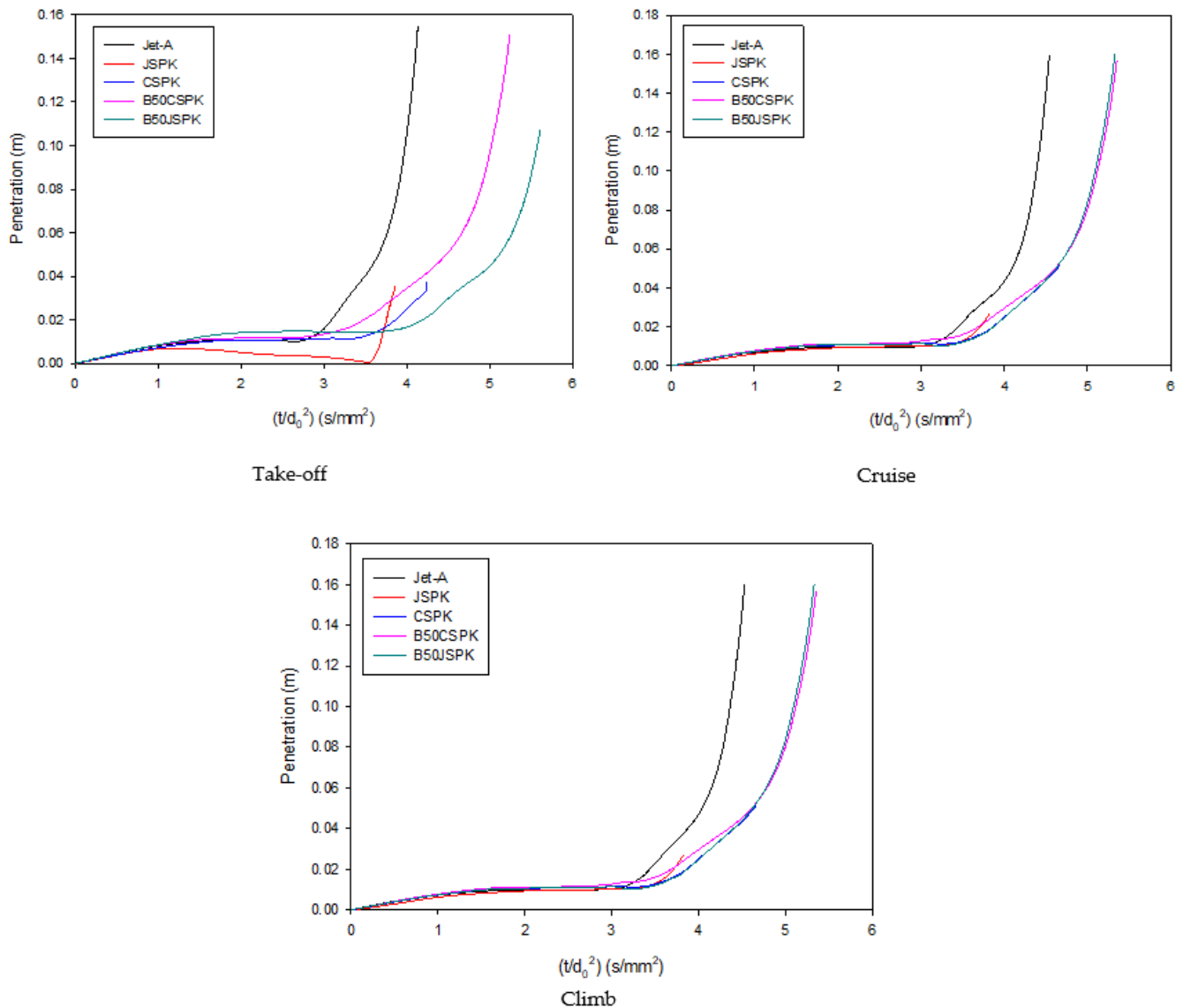


Figure 9. Penetration length of the fuel droplets.

Among the tested flight operating conditions, penetration of the spray is shorter during take-off than TOC and cruise. As expected, an insignificant difference in droplet penetration during cruise and TOC is observed mainly due to a slight difference in HPT rotational speed. The effect of altitude and Mach number is more dominant during take-off as they influence the chamber's inlet conditions. At low altitudes, the temperature, pressure, and density of the ambient air are higher than at higher altitudes. Consequently, the ambient conditions (pressure, temperature, and density) of the incoming air entering the combustion chamber during take-off are higher than at TOC and cruise. Higher air pressure entering the chamber promotes the lower spray penetration. The higher air pressure tends to increase the angle of the spray, allowing more air resistance, thus reducing the penetration. A similar observation was found in Vajda and Lešnik [33], who observed shorter spray penetration and a wider cone angle at higher ambient pressure.

Besides air pressure, air density also influences penetration length, as reported in Gogos and Soh [34]. The length of penetration was observed based on the spray cone angle. Guo and Jin [35] reported that a wider spray cone angle was observed as ambient air density decreases due to low air pressure. However, their finding has contradicted the finding obtained in the present study. In their study, temperature changes were not considered. According to the ideal gas equation, $P = \rho RT$, density is proportional to pressure and inversely

proportional to the temperature. Without considering the temperature, the ambient air becomes denser as the pressure increases. The particle resists moving further in denser air because high friction exists between the particle and the air molecules. As a result, a narrow cone angle was created, which consequently increases the penetration length. In this present study, the temperature changes were taken into account. Therefore, the influence of air density on the penetration length was not observed clearly. Air temperature during take-off is higher than the temperature during TOC and cruise. As the temperature increases, it eases the process of the particle to change from liquid to gaseous, thus reducing the length of the penetration.

Despite air properties, the density and viscosity of the fuel are crucial parameters to the penetration length. Lim and Razak [6] reported that the penetration of the spray corresponds to the higher ratio of air to fuel density, $\tilde{\rho} = \frac{\rho_a}{\rho_f}$. At constant air density, density of the fuel provides a significant impact on the penetration length. The effect of fuel density on the penetration observed in this present study is consistent with [6,36]. At a specific (t/d_0^2) , Figure 9 depicts that at all flight conditions, Jet-A penetrates longer than biofuels due to its higher density (Table 1). Moreover, the longer penetration of Jet-A is also influenced by the higher viscosity of the fuel. Viscous fuel provides a smaller spray cone angle due to the higher friction force in the viscous liquid. As the penetration of the spray is associated with the spray cone angle, the smaller cone angle therefore provided by the viscous liquid will increase the penetration length. However, a lower penetration is found when the biofuels are blended with Jet-A.

4. Conclusions

This study compares characteristics of biofuel spray with Jet-A by considering the combination of fuel properties and combustion inlet parameters that represent real flight operating conditions, namely take-off, top of climb (TOC), and cruise. This study expands the previous works that only focus on one particular condition (e.g., cruise only) to evaluate the performance of biofuels. By incorporating fuel properties and actual combustor inlet parameters, the evaluation of spray characteristics is more robust and reliable. The study was performed in two phases which represent each objective. The first objective is achieved in the first phase of the work which involved an engine simulation using GSP to obtain flow properties at the combustor inlet. Meanwhile, the second objective is achieved in the second phase of the work, which involved a simulation using ANSYS Fluent to simulate characteristics of the biofuels spray by incorporating fuel properties and combustor inlet data obtained from GSP simulation.

As for the first objective of this present study, it is concluded that at a specific fuel type, the results obtained from GSP simulation show insignificant differences in air pressure, air temperature, airflow, and fuel flow between TOC and cruise due to slight differences in rotational speed. The only differences were observed at take-off, mainly due to the lower altitude that affects the air characteristics entering the engine. As a result, a slight difference in thrust, TSFC, and spray penetration is observed for TOC and cruise, but vice versa at take-off. Meanwhile, at a specific flight operating condition, utilising biofuel in aircraft engines has improved TSFC. The amount of fuel consumed by the engine is lower for biofuel compared to Jet-A. Thus, at the constant amount of thrust, lower fuel consumed by the engine improves TSFC and efficiency of the engine. This result indicates that the engine consumed less fuel when operated with JSPK compared to other biofuels because of the low density of the fuel. The study observed that JSPK consumed 2.86% of fuel lower than Jet-A, which resulted from a 3.35% lower density compared to Jet-A.

As for the second objective of this study, it is concluded that at a specific fuel type, a tremendous impact of airflow characteristics in the combustor inlet on spray penetration is observed. The penetration is lower at take-off (lower altitude) due to higher air pressure that promotes the larger spray angles, which reduce the penetration of the spray. In addition, a higher air temperature at lower altitudes improves the transition of liquid fuel to gaseous during the evaporation and vaporisation process which resulted in a lower penetration

length. In addition, by concentrating on a specific fuel flight operating condition, this study observed the relationship between density and viscosity of the fuels on penetration length. The penetration of Jet-A is higher due to its higher density and viscosity compared to biofuels. Higher density and viscosity produce smaller cone angles as the fuels sprayed into the chamber, thus prolonging the penetration length. However, blending Jet-A with biofuel shortened penetration length as the critical fuel properties influencing penetration length were improved.

Various factors are affecting the performance of the engine. However, as far as this present study is concerned, it is found that utilising biofuels in the engine provides up to a 15% reduction in maximum flame temperature and up to an 83% reduction of penetration length when compared to Jet-A. Among the biofuels, JSPK provides excellent performance for the engine at all flight operating conditions. For that reason, this study concluded that regardless of the changes needed for the chamber, JSPK has the potential to substitute Jet-A due to its capability to produce similar thrust with Jet-A, but with lower fuel consumption and faster droplet reduction that indicates a better evaporation rate.

The current evaluation of combustion characteristics in this study is based on the global stoichiometric reaction of fuel and air due to the limitation of reduced chemical reaction mechanisms of the tested biofuels. The implementation of reduced chemical reaction mechanisms can improve the results and reliability of the fuels over a wide range of flow speeds and temperature conditions. For this purpose, further development of biofuel combustion performance is essential. In addition, further research on the computational model of gas emissions in every primary manoeuvre is crucial to predict the total emissions of the aeroplane throughout a trip.

Author Contributions: Conceptualization; methodology; supervision; validation and funding acquisition, N.M.M.; software; investigation; data curation; writing—original draft preparation, S.S.M.; writing—review and editing, N.M.M., A.A.A.R. and M.S.Z.A. All authors have read and agreed to the published version of the manuscript.

Funding: Acknowledgement to Ministry of Higher Education Malaysia for Fundamental Research Grant Scheme with Project Code: FRGS/1/2019/TK07/USM/03/5.

Institutional Review Board Statement: Not Applicable.

Informed Consent Statement: Not Applicable.

Data Availability Statement: Data available in a publicly accessible repository.

Conflicts of Interest: The authors declare no conflict of interest.

References

1. Dong, Q.; Chen, F.; Chen, Z. Airports and air pollutions: Empirical evidence from China. *Transp. Policy* **2020**, *99*, 385–395. [CrossRef]
2. ICAO. The World of Air Transport. 2019. Available online: <https://www.icao.int/annual-report-2019/Pages/the-world-of-air-transport-in-2019.aspx> (accessed on 26 August 2021).
3. Bhele, S.; Deshpande, N.; Thombre, S. Experimental Investigations on Combustion Characteristics of Jatropha biodiesel (JME) and its Diesel Blends for Tubular Combustor Application. *J. Adv. Automob. Eng.* **2016**, *5*, 2.
4. Prussi, M.; O’Connell, A.; Lonza, L. Analysis of current aviation biofuel technical production potential in EU28. *Biomass Bioenergy* **2019**, *130*, 105371. [CrossRef]
5. Zhang, P.; Su, X.; Yi, C.; Chen, H.; Xu, H.; Geng, L. Spray, atomization and combustion characteristics of oxygenated fuels in a constant volume bomb: A review. *J. Traffic Transp. Eng.* **2020**, *7*, 282–297. [CrossRef]
6. Lim, J.; Razak, N.A.; Mazlan, N.M. An evaluation of alternative fuels’ spray penetration at various spray cone angles and injection pressures using a simple evaporation model. *Biofuels* **2019**, *2019*, 1–11. [CrossRef]
7. Won, J.; Baek, S.W.; Kim, H. Autoignition and combustion behavior of emulsion droplet under elevated temperature and pressure conditions. *Energy* **2018**, *163*, 800–810. [CrossRef]
8. Tucki, K.; Mruk, R.; Orynych, O.; Gola, A. The effects of pressure and temperature on the process of auto-ignition and combustion of rape oil and its mixtures. *Sustainability* **2019**, *11*, 3451. [CrossRef]
9. Shameer, P.M.; Ramesh, K. Assessment on the consequences of injection timing and injection pressure on combustion characteristics of sustainable biodiesel fuelled engine. *Renew. Sustain. Energy Rev.* **2018**, *81*, 45–61. [CrossRef]

10. Ganji, P.R.; Raju, V.R.K.; Rao, S.S. Effect of Fuel Injection Pressure and Spray Cone Angle in DI Diesel Engine Using CONVERGETM CFD Code. *Procedia Eng.* **2015**, *127*, 295–300. [[CrossRef](#)]
11. Zhu, L.; Luo, F.; Qi, Y.-Y.; Wei, M.; Ge, J.-R.; Liu, W.-L.; Li, G.-L.; Jen, T.C. Effects of spray angle variation on mixing in a cold supersonic combustor with kerosene fuel. *Acta Astronaut.* **2018**, *144*, 1–11. [[CrossRef](#)]
12. Allouis, C.; Amoresano, A.; Capasso, R.; Langella, G.; Niola, V.; Quaremba, G. The impact of biofuel properties on emissions and performances of a micro gas turbine using combustion vibrations detection. *Fuel Process. Technol.* **2018**, *179*, 10–16. [[CrossRef](#)]
13. Kannaiyan, K.; Sadr, R. Experimental investigation of spray characteristics of alternative aviation fuels. *Energy Convers. Manag.* **2014**, *88*, 1060–1069. [[CrossRef](#)]
14. Varatharajan, K.; Cheralathan, M. Influence of fuel properties and composition on NO_x emissions from biodiesel powered diesel engines: A review. *Renew. Sustain. Energy Rev.* **2012**, *16*, 3702–3710. [[CrossRef](#)]
15. Shin, J.; Kim, D.; Seo, J.; Park, S. Effects of the physical properties of fuel on spray characteristics from a gas turbine nozzle. *Energy* **2020**, *205*, 118090. [[CrossRef](#)]
16. Zhou, L.; Liu, Z.-W.; Wang, Z.-X. Numerical study of influence of biofuels on the combustion characteristics and performance of aircraft engine system. *Appl. Therm. Eng.* **2015**, *91*, 399–407. [[CrossRef](#)]
17. Mazlan, N.M.; Savill, M.; Kipouros, T. Computational evaluation and exploration of combustion performance for liquid jet fuels derived from biomass. In Proceedings of the 3rd CEAS Air & Space Conference, San Giorgio Maggiore Island, Venice, Italy, 24–28 October 2011.
18. Azami, M.H.; Savill, M. Modelling of spray evaporation and penetration for alternative fuels. *Fuel* **2016**, *180*, 514–520. [[CrossRef](#)]
19. Rubie, J.S.; Li, Y.G.; Jackson, A.J.B. Performance Simulation and Analysis of a Gas Turbine Engine Using Drop-In Bio-Fuels. In *Turbo Expo: Power for Land, Sea, and Air*; American Society of Mechanical Engineers: New York, NY, USA, 2018; Volume 51043, p. V003T06A005.
20. Yilmaz, N.; Atmanli, A. Sustainable alternative fuels in aviation. *Energy* **2017**, *140*, 1378–1386. [[CrossRef](#)]
21. Mazlan, N.M.; Savill, M.; Kipouros, T. Evaluating NO_x and CO emissions of bio-SPK fuel using a simplified engine combustion model: A preliminary study towards sustainable environment. *Proc. Inst. Mech. Eng. Part G J. Aerosp. Eng.* **2017**, *231*, 859–865. [[CrossRef](#)]
22. Mazlan, N.M.; Savill, M.; Kipouros, T. Effects of biofuels properties on aircraft engine performance. *Aircr. Eng. Aerosp. Technol. Int. J.* **2015**, *87*, 437–442. [[CrossRef](#)]
23. Sivakumar, D.; Vankeswaram, S.K.; Sakthikumar, R.; Raghunandan, B.N.; Hu, J.T.C.; Sinha, A.K. An experimental study on jatropa-derived alternative aviation fuel sprays from simplex swirl atomizer. *Fuel* **2016**, *179*, 36–44. [[CrossRef](#)]
24. Hashimoto, N.; Nishida, H.; Ozawa, Y. Fundamental combustion characteristics of Jatropa oil as alternative fuel for gas turbines. *Fuel* **2014**, *126*, 194–201. [[CrossRef](#)]
25. Mark, C.P.; Selwyn, A. Design and analysis of annular combustion chamber of a low bypass turbofan engine in a jet trainer aircraft. *Propuls. Power Res.* **2016**, *5*, 97–107. [[CrossRef](#)]
26. Kinder, J.; Rahmes, T. Evaluation of Bio-Derived Synthetic Paraffinic Kerosene (Bio-SPK). The Boeing Company Sustainable Biofuels Research & Technology Program. 2009. 16 p.–[Электронный ресурс]. Режим доступа. Available online: <http://www.safug.org/assets/docs/biofuel-testing-summary.pdf> (accessed on 26 August 2021).
27. Mazlan, N.M.; Savill, M.; Kipouros, T.; Li, Y.-G. A numerical study into the effects of bio-synthetic paraffinic kerosene blends with jet-A fuel for civil aircraft engine. In Proceedings of the ASME Turbo Expo 2012: Turbine Technical Conference and Exposition, Copenhagen, Denmark, 11–15 June 2012; American Society of Mechanical Engineers: New York, NY, USA, 2012; pp. 165–173.
28. Li, R.; Guo, Y.; Nguang, S.K.; Chen, Y. Takagi-Sugeno fuzzy model identification for turbofan aero-engines with guaranteed stability. *Chin. J. Aeronaut.* **2018**, *31*, 1206–1214. [[CrossRef](#)]
29. Gaspar, R.M.P.; Sousa, J.M.M. Impact of alternative fuels on the operational and environmental performance of a small turbofan engine. *Energy Convers. Manag.* **2016**, *130*, 81–90. [[CrossRef](#)]
30. Peric, M.; Ferguson, S. The Advantage of Polyhedral Meshes. p. 2. Available online: <https://www.semanticscholar.org/paper/The-advantage-of-polyhedral-meshes-Peri%20C4%87-Ferguson/51ae90047ab44f53849196878bfec4232b291d1c> (accessed on 1 July 2021).
31. Mattingly, J.D. *Elements of Propulsion: Gas Turbines and Rockets*; American Institute of Aeronautics and Astronautics: Reston, VA, USA, 2006.
32. Chin, J.; Lefebvre, A. The role of the heat-up period in fuel drop evaporation. *Int. J. Turbo Jet Engines* **1985**, *2*, 315–326. [[CrossRef](#)]
33. Vajda, B.; Lešnik, L.; Bombek, G.; Biluš, I.; Žunič, Z.; Škerget, L.; Hočevar, M.; Širok, B.; Kegl, B. The numerical simulation of biofuels spray. *Fuel* **2015**, *144*, 71–79. [[CrossRef](#)]
34. Gogos, G.; Soh, S.; Pope, D.N. Effects of gravity and ambient pressure on liquid fuel droplet evaporation. *Int. J. Heat Mass Transf.* **2003**, *46*, 283–296. [[CrossRef](#)]
35. Guo, Z.; Jin, Y.; Zhang, K.; Yao, K.; Wang, Y.; Wu, D.; He, X.; Zheng, M. Effect of Low Ambient Pressure on Spray Cone Angle of Pressure Swirl Atomizer. *Int. J. Aerosp. Eng.* **2021**, *2021*, 5539231. [[CrossRef](#)]
36. Mei, S.S.; Mazlan, N.M. Evaluation of Combustion Characteristics on Simple Cylindrical Combustion Chamber for Different Operating Conditions and Alternative Fuels. In *Proceedings of International Conference of Aerospace and Mechanical Engineering*; Springer: Singapore, 2019; pp. 317–327.